Sensors and Actuators B 211 (2015) 111–115

Contents lists available at ScienceDirect

Sensors and Actuators B: Chemical

journal homepage: www.elsevier.com/locate/snb

Enhanced photoelectrochemical and sensing performance of novel TiO_2 arrays to H_2O_2 detection

Lianqing Yu[a,*], Yaping Zhang[a,*], Qianqian Zhi[a], Qingqing Wang[a], Forrest S. Gittleson[b], Jinyang Li[b], André D. Taylor[b]

[a] *College of Science and Key Laboratory of New Energy Physics & Materials Science, China University of Petroleum, QingDao, China*
[b] *Department of Chemical and Environmental Engineering, Yale University, New Haven, CT 06511, United States*

ARTICLE INFO

Article history:
Received 11 September 2014
Received in revised form
20 December 2014
Accepted 9 January 2015
Available online 28 January 2015

Keywords:
Silver
TiO_2 NW arrays
Photodeposition
Photoelectrochemical property

ABSTRACT

Ag-decorated TiO_2 nanowire arrays were facilely prepared by H_2O_2 corrosion of Ti and subsequent photodeposition of Ag. Array structures and photoelectric properties were characterized by X-ray diffraction (XRD), scanning electron microscopy (SEM), UV–vis absorption spectroscopy and electrochemical methods. These results show that Ag quantum dots are evenly distributed on the surface of TiO_2 nanowires. With an Ag content of 0.4 at%, the electrode's photocurrent density and photoconversion efficiency obtained optimum values of 0.29 mA/cm^2 and 8.55%, respectively. The enhanced photoelectrochemical properties with Ag modification can be attributed to the extended visible light absorption range and improved separation of photo-generated carriers. Additionally, the modified nanowire arrays exhibited much stronger photoelectrocatalytic reduction activity toward hydrogen peroxide in comparison with pure TiO_2 arrays or previously reported Ag electrodes.

1. Introduction

In recent years, TiO_2 material has attracted great interest for environmental applications [1,2], especially in the field of photocatalytic degradation of organic pollutants, because of its biological and chemical inertness, nontoxicity, strong anti-oxidizing power and long-term stability against light. However, commercial application of photocatalytic super fine TiO_2 nanoparticles (NPs) is greatly limited due to the difficulty of recycling this material. TiO_2 nanostructures on Ti metal substrates prepared by either direct oxidation [3–5] or an anodic oxidation method [6] can overcome this obstacle and demonstrate good photoelectrochemical (PEC) and photocatalytic properties. Simultaneously, in comparison with one-dimensional nanostructures of rod and tube, titania nanowire (NW) arrays have been confirmed to possess an advantage in charge separation over compact films [4], which is of great importance for photocatalysts and photoanodes.

A wide band gap and high recombination rate for photo-generated electrons and holes with TiO_2 are obstacles to photoelectric application. In order to improve the PEC activity of TiO_2 [7,8] various modifications have been demonstrated including with pure metal [9,10] or non-metal dopants [11], or surface modification with semiconductors [12–14]. Thanks to its high carrier transfer rate and plasmonic effect, Ag deposited on a TiO_2 surface successfully acts as a transfer intermediate for photo-generated electrons and holes, promoting charge carrier separation [15,16]. With a view toward controlling Ag particle size and dispersion, methods of sol–gel [17–20] and photodeposition [21,22] can be used since photocatalytic activity closely depends on content, crystal size, and morphology [23–26]. Specifically, Ag quantum dots and/or nanoclusters can effectively promote the separation of the photo-generated electrons and holes [23]. However, there are still few efforts and little attention paid on the PEC properties and mechanisms of structures like Ag quantum dots modified TiO_2 NW arrays.

In the electrochemical biosensor field, amperometric detection of H_2O_2 provides a signal transduction to indirectly recognize biomolecules such as glucose, cholesterol, and acetylcholine with oxidase modified electrodes [27–33]. Silver has previously been used in electrochemical detectors for H_2O_2, which could exhibit strong cytotoxicity toward a broad range of microorganisms [34] and has shown remarkably low toxicity compared to other heavy metal elements. In this work, we combined the excellent electrocatalytic properties of Ag quantum dots and the photocatalytic activities of TiO_2 NW arrays. The resulting Ag/TiO_2 array electrodes were characterized by size, structure, PEC activity as well as H_2O_2 biosensor behaviors to demonstrate the role of both Ag quantum dots and TiO_2 NW arrays.

---

[*] Corresponding authors: Tel.: +86 0532 86983372; fax: +86 0532 86983372.
E-mail address: iyy2000@163.com (L. Yu).

http://dx.doi.org/10.1016/j.snb.2015.01.060
0925-4005/

2. Experimental

2.1. Preparation of TiO_2 NW arrays

Ti foils (2.0 cm × 1.0 cm × 0.2 mm) were first cleaned for 15 min by sonication in acetone and anhydrous ethanol, respectively. Then the dried Ti foil was put into an autoclave filled with 50 ml of H_2O_2. The autoclave was put in a preheated blast electric oven at 80 °C for 6 h and then cooled to room temperature. The sample was washed with distilled water three times before annealing at 450 °C for 2 h.

2.2. Preparation of Ag/TiO_2 arrays

Ag quantum dots modified TiO_2 arrays were prepared by a photodeposition method. TiO_2 NW arrays were immersed for 30 min in $AgNO_3$ solution (5 mM, 10 mM, 15 mM, 20 mM) and marked as 5 mM Ag/TiO_2, 10 mM Ag/TiO_2, 15 mM Ag/TiO_2, and 20 mM Ag/TiO_2, respectively. Then Ag/TiO_2 arrays were illuminated with a xenon lamp for 4 min to induce Ag reduction.

2.3. Characterization of samples

The phase of TiO_2 arrays was determined by X-ray diffraction (XRD) performed on an X-ray diffractometer (Model Dmax-2700, Dandong Fangyuan instrument Co., Ltd., Dandong, China.) with Cu Kα radiation at 40 kV and 30 mA. The morphologies were investigated with a scanning electron microscope (FESEM, model S-4800, Hitachi Ltd., Shanghai, China). UV–vis absorption spectra were recorded using a Shimadzu UV-2450 spectrophotometer.

2.4. Measurements of PEC properties and H_2O_2 sensing

PEC performances and Mott–Schottky (MS) spectra of the as-prepared samples were measured with a CHI760D electrochemical workstation in a quartz beaker using a three-electrode system with a platinum wire as a counter electrode and a saturated calomel electrode (SCE) as a reference electrode. 1 M of KOH was used as electrolyte. The working electrode was illuminated with a 350 W xenon lamp under a light power density of 35 mW/cm^2. The photocurrent was recorded concurrently with the light switching on and off without applied voltage.

Photocurrent of the H_2O_2 detection sensor was obtained by a three-electrode system in a stirred 0.1 M phosphate buffer (PBS) solution by applying a potential of 0.15 V to the sample. The concentration of H_2O_2 was increased by 2.5 mM after testing every 50 s by injection.

3. Results and discussion

3.1. Characterization

Fig. 1 shows the XRD patterns of Ag/TiO_2 arrays. All diffraction peaks of the Ag-modified TiO_2 arrays can be indexed as Ti (JCPDS 65-6231) or the anatase phase of TiO_2 (JCPDS 21-1272). In addition, no characteristic peaks of Ag were detected, which was likely due to the low concentration and well dispersed nature of Ag quantum dots on the TiO_2 NW arrays.

Fig. 2 shows SEM images of free and Ag modified TiO_2 NW arrays. The anatase TiO_2 has a well-defined NW array structure, with a length of more than 500 nm and a diameter of approximately 20 nm. No obvious structural changes were observed on the morphology of Ag/TiO_2 NW arrays after Ag quantum dots deposition at size of 5–10 nm (Fig. 2(b)). Energy-dispersive X-ray spectroscopy (EDS) indicated Ag content of 0.4 at% for the 10 mM Ag/TiO_2 array sample.

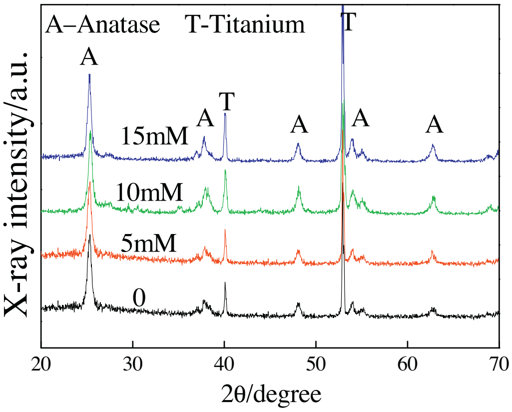

Fig. 1. XRD pattern of Ag/TiO_2 arrays made with different concentrations of Ag precursor.

Table 1
Photoelectric performance of different Ag concentrations.

$AgNO_3$ concentration (mM)	Deposit amount (at%)	Photocurrent densities (mA/cm^2)	Photoconversion efficiency (%)
0	0	0.10	2.69
5	0.19	0.15	4.21
10	0.40	0.29	8.55
15	0.63	0.26	7.47
20	0.82	0.20	5.33

The UV–vis absorption spectra of TiO_2 and Ag/TiO_2 NW arrays are shown in Fig. 2(d). The absorption edge of the pure TiO_2 NW arrays is observed at around 410 nm, corresponding to a band-gap energy of 3.12 eV. After the deposition of Ag, the absorption edge is shifted significantly toward the visible region to 468.2 nm, which can be attributed to the surface plasmon resonance absorption of Ag quantum dots. The adsorption wavelength of Ag/TiO_2 NW was much higher than that of TiO_2 (∼410 nm) or previous reported Ag/TiO_2 (∼440 nm) [35].

3.2. PEC properties under xenon light illumination

Fig. 3(a) shows the transient photocurrent responses of TiO_2 arrays with Ag quantum dots modification. Upon xenon light illumination, the photocurrent increases with Ag photodeposited on the TiO_2 NW arrays (seen in Table 1). The highest photocurrent density was obtained at 0.29 mA/cm^2 for NW arrays with 0.4 at% Ag content. We believe that the plasmon resonance effect of Ag quantum dots enhances the transfer and lifetime of photogenerated electrons and significantly improves the PEC activity of TiO_2 NWs. However, over-deposition of silver will cover and shield the TiO_2 surface from the light. This results in a decrease in the number of generated photoelectrons and holes; therefore the photocurrent decreases with Ag concentrations higher than 10 mM. After calculation (according to our previous report [36]) the photoconversion efficiency from light energy to chemical energy remarkably improved from 2.69% to 8.55% (Fig. 3(b)), after Ag quantum dots modification on TiO_2 NW arrays.

Fig. 4 represents Nyquist diagrams from electrochemical impedance spectroscopy (EIS) for different samples obtained in dark and under light illumination. It reveals the relationship between the real part (Z′) and the imaginary part (Z″) of the Ag/TiO_2 NW array electrodes. The equivalent circuit for this cell system is depicted in the inset of Fig. 4. In the equivalent circuit, R_b is the bulk resistance of the electrolyte, separator, and electrode, corresponding to the resistance value of the high frequency intercept of the semicircle with the real axis. C_{dl} and R_{ct} are the double